Published in final edited form as:
Cell. 2013 August 29; 154(5): 1085–1099. doi:10.1016/j.cell.2013.07.035.

Beclin 2 Functions in Autophagy, Degradation of G Protein-Coupled Receptors, and Metabolism

Congcong He[1,2,4], **Yongjie Wei**[1,2,4], **Kai Sun**[3,4], **Binghua Li**[4], **Xiaonan Dong**[2,4], **Zhongju Zou**[1,2,4], **Yang Liu**[2,4], **Lisa N. Kinch**[1,5,6], **Shaheen Khan**[4], **Sangita Sinha**[9], **Ramnik J. Xavier**[10,11,12], **Nick V. Grishin**[1,5,6], **Guanghua Xiao**[7], **Eeva-Liisa Eskelinen**[13], **Philipp E. Scherer**[3,4], **Jennifer L. Whistler**[14], and **Beth Levine**[1,2,4,8,#]

[1]Howard Hughes Medical Institute University of Texas Southwestern Medical Center, Dallas, TX 75390 USA [2]Center for Autophagy Research University of Texas Southwestern Medical Center, Dallas, TX 75390 USA [3]Touchstone Diabetes Center University of Texas Southwestern Medical Center, Dallas, TX 75390 USA [4]Department of Internal Medicine University of Texas Southwestern Medical Center, Dallas, TX 75390 USA [5]Department of Biochemistry University of Texas Southwestern Medical Center, Dallas, TX 75390 USA [6]Department of Biophysics University of Texas Southwestern Medical Center, Dallas, TX 75390 USA [7]Department of Clinical Sciences University of Texas Southwestern Medical Center, Dallas, TX 75390 USA [8]Department of Microbiology, University of Texas Southwestern Medical Center, Dallas, TX 75390 USA [9]Department of Chemistry and Biochemistry, North Dakota State University, ND 58102 USA [10]Center for Computational and Integrative Biology [11]Gastrointestinal Unit, Massachusetts General Hospital, Harvard Medical School, Boston, MA 02114 USA [12]Broad Institute of Harvard and Massachusetts Institute of Technology, Cambridge, MA 02142 USA [13]Department of Biosciences, Division of Biochemistry and Biotechnology, University of Helsinki, Helsinki, FI-00014 Finland [14]Ernest Gallo Clinic and Research Center, University of California San Francisco, Emeryville, CA 94608 USA

Summary

The molecular mechanism of autophagy and its relationship to other lysosomal degradation pathways remain incompletely understood. Here, we identified a previously uncharacterized mammalian-specific protein, Beclin 2, which like Beclin 1, functions in autophagy and interacts with class III PI3K complex components and Bcl-2. However, Beclin 2, but not Beclin 1, functions in an additional lysosomal degradation pathway. Beclin 2 is required for ligand-induced endolysosomal degradation of several G protein-coupled receptors (GPCRs) through its interaction with GASP1. *Beclin 2* homozygous knockout mice have decreased embryonic viability, and heterozygous knockout mice have defective autophagy, increased levels of brain cannabinoid 1 receptor, elevated food intake, and obesity and insulin resistance. Our findings identify Beclin 2 as a novel converging regulator of autophagy and GPCR turnover, and highlight

[#]To whom correspondence should be addressed: beth.levine@utsouthwestern.edu.
[*]These authors contributed equally

Supplemental Information: Supplemental Information includes Extended Experimental Procedures and seven figures.

Accession Numbers: Human *beclin 2*: NG_022940; mouse *beclin 2*: NG_028451

the functional and mechanistic diversity of Beclin family members in autophagy, endolysosomal trafficking and metabolism.

Introduction

Autophagy is a lysosomal degradation pathway that functions in nutrient recycling, energy generation, and the clearance of damaged proteins and organelles (Mizushima and Komatsu, 2011). This homeostatic pathway is conserved in all eukaryotes, and orthologs of a core set of essential genes, the *au*toph*agy*-related (Atg) genes, have been discovered in organisms ranging from yeasts to humans (Chen and Klionsky, 2011). During the evolution of higher eukaryotes, many autophagy genes (such as *Atg8* and *Atg1*) have been duplicated, but the functional importance of such duplication is not fully understood. In theory, the duplicated genes may carry out new functions that convey temporal-spatial specificity in multicellular organisms, fine-tune autophagic activity at different levels, and/or mediate cross-talk between autophagy and other biological pathways. The increased complexity in the autophagy machinery in higher eukaryotes may enhance the ability of such organisms to respond and adapt to complex environmental signals.

It is possible that autophagy gene duplication evolved in part to permit the integration of different lysosomal degradation pathways. In addition to autophagy (which targets intracellular components for degradation), cargos from extracellular sources (such as plasma membrane proteins that cycle through endocytic vesicles and bacteria and apoptotic corpses that are captured by phagocytosis) can be transported to lysosomes for degradation. Several autophagy proteins function in phagocytosis and apoptotic corpse clearance (such as Beclin 1, Atg5, Atg7, and LC3) (Levine et al., 2011) and components of the Beclin 1/class III PI3K autophagy complex regulate endocytic degradation of the epidermal growth factor receptor (EGFR) tyrosine kinase (Funderburk et al., 2010). In addition to the role of autophagy proteins in targeting cargo from different sources to the lysosome, there is also overlap between the autophagy machinery and proteins involved in other endosomal sorting pathways; for example, the yeast genes, *VPS15*, *VPS34*, and *ATG6/VPS30* (the yeast ortholog of mammalian *beclin 1*) are required both for autophagy and efficient endosome-to-Golgi retrograde transport (Funderburk et al., 2010).

The lysosomal degradation of G protein-coupled receptors (GPCRs), the largest family of cell surface receptors encoded in the human genome, represents a key mechanism for controlling cellular responses to environmental cues (Hanyaloglu and von Zastrow, 2008). Following ligand-induced activation, internalized GPCRs may undergo different fates which produce distinct effects on cellular signaling, including endocytic sorting to a recycling pathway that results in rapid signal resensitization, or endocytic sorting to the lysosome that results in permanent signal termination. The best-studied mechanism for post-endocytic sorting of GPCRs to the lysosome involves the ESCRT (endosomal sorting complex required for transport) machinery (Hurley and Emr, 2006), which mediates the targeting of ubiquitinated cargo to the yeast vacuole/mammalian lysosome via an endocytic intermediate compartment called the multivesicular body. There is also evidence that non-ESCRT proteins contribute to GPCR sorting to mammalian lysosomes. One family of such proteins

are the GPCR-associated sorting proteins, GASP1 and GASP2, that associate with a broad range of seven transmembrane-spanning GPCRs (Moser et al., 2010). GASP1 has been shown to regulate the degradation of several GPCRs that traffic to lysosomes after agonist-induced endocytosis, including the delta opioid receptor (DOR), cannabinoid 1 receptor (CB1R), dopamine D2 receptor, bradykinin 1 receptor, and a non-recycling mutant of the β-adrenergic receptor (β-ala). Despite the overlap between the autophagy machinery and proteins involved in vacuolar protein sorting and in certain lysosomal degradation pathways, it is not yet known whether any autophagy proteins participate in agonist-induced lysosomal degradation of GPCRs.

Here, we characterize a new autophagy gene homolog, *beclin 2*, which also functions in the ligand-induced degradation of GASP1-regulated GPCRs. These findings identify a hitherto unappreciated level of integration between two distinct lysosomal degradation pathways that exert crucial roles in eukaryotic biology.

Results

Identification of Beclin 2, a New Beclin Family Member Involved in Autophagy

Based upon a BLAST search of the human and mouse database, we identified novel mammalian-specific genes, NG_022940 and NG_028451, which encode a predicted 431 amino acid, 49 kDa human protein and a predicted 447 amino acid, 50 kDa mouse protein which share 57% and 44% sequence identity (human and mouse, respectively) with the essential autophagy and tumor suppressor protein, Beclin 1 (Figure 1A). Similar to Beclin 1, this predicted protein contains a BH3 domain, a central coiled-coil domain and a C-terminal evolutionarily conserved domain. Based on this similarity in sequence and domain organization, we concluded that NG_022940 and NG_028451 represent novel members of the Beclin family, and therefore, named NG_022940 human Beclin 2 and NG_028451 mouse Beclin 2.

Beclin 2 subfamily members are mammalian-specific; Beclin 1 subfamily members are present in more primitive vertebrates (such as fish) (Figure 1A); and, at least based on multiple sequence alignments, Atg6/Beclin orthologs in invertebrate organisms (such as *S. cerevisiae*, *C. elegans*, *D. melanogaster*, *A. thaliana*) cannot be classified as either Beclin 1 or Beclin 2 (Figure S1 and data not shown). Although there is a high level of amino acid sequence similarity between mammalian Beclin 1 and Beclin 2, the genomic organization of *beclin 1* and *beclin 2* are quite different. Mouse and human *beclin 1* have twelve exons, whereas mouse *beclin 2* contains only one intron and the human counterpart is intronless. Human *beclin 2* maps to chromosome 1q43 near the autophagy gene, MAP1LC3C, and the genomic location of mouse *beclin 2* (chromosome 1 H4) is syntenic to that of human *beclin 2*.

We analyzed levels of mouse and human mRNA and protein expression in selected tissues. We detected mouse *beclin 2* mRNA expression in multiple organs including brain, skeletal muscle, placenta, thymus and uterus, and more weakly in liver, testis, stomach, and 17 day-old embryos (Figure 1B). We also detected human Beclin 2 protein expression (predicted molecular weight 49 kD; apparent molecular weight 53 kD) in samples from human fetal

and adult brains using an antibody generated against amino acids 49-67 of human Beclin 2 (Figure 1C). We confirmed the specificity of this antibody by showing that siRNA directed against *human beclin 2* decreased protein expression of human Beclin 2, but not human Beclin 1 in HeLa cells (Figure 2A) and HEK293 cells (Figure S3). The detection of mouse and human *beclin 2* mRNA and protein expression provides biological evidence that the database classification of NG_022940 and NG_028451 as pseudogenes is incorrect.

The Beclin family member, Beclin 1, an ortholog of yeast Atg6, is required for mammalian autophagy (Chen and Klionsky, 2011). To determine if Beclin 2 also functions in autophagy, we evaluated the effects of an siRNA that specifically targets Beclin 2 (Fig. 2A, Fig. S2A) on basal and starvation-induced autophagy in HeLa cells using three well-established assays (Mizushima et al., 2010): degradation of p62, an autophagy substrate; detection of GFP-LC3 puncta (autophagosomes); and conversion of the non-lipidated form of LC3 (LC3-I) to the phosphatidylethanolamine-conjugated form (LC3-II). Although many studies measure autophagy by examining LC3-II conversion, it should be noted that several autophagy proteins, including yeast Atg6 and mammalian Beclin 1, are not required for LC3 lipidation but are required for autophagosome formation (Mizushima et al., 2010).

During normal growth conditions, *beclin 2* siRNA knockdown in HeLa cells decreased numbers of GFP-LC3 puncta, decreased the ratio of LC3-II/LC3-I, and increased the total levels of LC3 (which is also substrate of autophagy), although no significant changes were observed in p62 levels (Figures 2B-2D and S2B). In response to amino acid starvation, both *beclin 1* and *beclin 2* siRNA knockdown resulted in decreased numbers of GFP-LC3 puncta, decreased conversion of LC3-I to LC3-II, and decreased p62 degradation (Figure 2B-2D and S2B). The decrease in autophagosomes in basal and starvation conditions was not due to an acceleration of autophagolysosomal maturation, as the number of autophagosomes was also decreased in *beclin 1* and *beclin 2* siRNA-treated cells in the presence of the lysosomal inhibitor, bafilomycin A1 (Figure 2D). Furthermore, changes in p62 or LC3 protein levels could not be attributed to indirect effects of the siRNAs on p62 or LC3 mRNA expression (Figure S2C). The effect of *beclin 2* (but not *beclin 1*) siRNA on basal and starvation-induced autophagy (as measured by numbers of GFP-LC3 puncta) was partially rescued by expression of a Beclin 2 siRNA non-targetable mutant rescue plasmid (Figure 2A, 2E, and S2A). The Beclin 2 siRNA non-targetable mutant plasmid also rescued starvation-induced autophagy in *beclin 2* knockdown cells as measured by p62 degradation and LC3-II conversion (Figure 2F). This suggests that the defect in autophagy is likely due to depletion of Beclin 2, rather than an off-target effect of *beclin 2* siRNA. Taken together, these data indicate that Beclin 2, like Beclin 1, functions in autophagy in human cells. Depending on the sensitivity of the assay, the effect can be observed in basal conditions as well as in starvation conditions. In addition, *beclin 2* siRNA blocked CCCP-induced Parkin-mediated mitophagy in HeLa cells (Figure S2D), indicating a role for Beclin 2 in selective autophagy.

Beclin 2 Interacts with Several Known Binding Partners of Beclin 1

We examined whether mouse and human Beclin 2 interact with known binding partners of Beclin 1 (Chen and Klionsky, 2011). Several components of the class III PI3K complex, including endogenous ATG14, AMBRA1, and VPS34 (which function in autophagosome

formation) and UVRAG (which functions in autophagosome maturation) immunoprecipitated with Flag epitope-tagged human Beclin 1, human Beclin 2 and mouse Beclin 2 (Figure 2G). The co-immunoprecipitation of AMBRA1 was significantly stronger with human or mouse Beclin 2 than with human Beclin 1. The Beclin 1-binding anti-autophagy protein, Bcl-2, co-immunoprecipitated with Flag epitope-tagged mouse and human Beclin 2 (Figure 2H); however, unlike with Beclin 1 (Pattingre et al., 2005), this interaction was not disrupted by starvation. No interaction was detected between mouse or human Beclin 2 and the Beclin 1-binding negative regulator of autophagy, Rubicon. Thus, Beclin 2 interacts with several of the known Beclin 1 binding partners, including ATG14, VPS34, AMBRA1, UVRAG, and Bcl-2. However, Beclin 1 and Beclin 2 differ somewhat with respect to binding affinities and/or regulation of certain protein-protein interactions with other autophagy-related proteins.

GASP1 Interacts with Beclin 2

The alignment of Beclin 2 with Beclin 1 (Figure 1A) revealed greater divergence at the N terminus as compared to the C terminus. This suggested that the N terminus of Beclin 2 might have a unique, autophagy-independent function. To identify unique interacting partners and functions of Beclin 2, we performed a yeast two-hybrid screen of a human brain cDNA library using the N-terminal 88 amino acids of human Beclin 2 as bait. Fourteen hits were isolated that mapped to the C terminus of a 230 kDa protein, G protein-coupled receptor associated sorting protein 1 (GASP1) (Figure 3A), which is required for agonist-induced lysosomal degradation of a subset of G protein-coupled receptors (GPCRs), including the DOR, CB1R, and a non-recycling mutant form of the β-adrenergic (β-Ala) receptor (Martini et al., 2007; Moser et al., 2010; Tappe-Theodor et al., 2007; Whistler et al., 2002). The N-terminal domain of Beclin 1 (amino acids 1-90) did not interact with any of the Beclin 2-interacting GASP1 fragments in a yeast two-hybrid interaction assay (data not shown).

We confirmed that GASP1 interacts with Beclin 2 in mammalian cells. Endogenous human GASP1 co-immunoprecipitated with Flag epitope-tagged human Beclin 2, but not human Beclin 1, in HEK293 cells (Figure 3B). Similarly, endogenous mouse GASP1 co-immunoprecipitated strongly with Flag epitope-tagged mouse Beclin 2, but only weakly with Beclin 1, in mouse Neuro2A cells (Figure 3C). The interaction between Beclin 2 and GASP1 is species-specific, as no interaction between human GASP1 and mouse Beclin 2 was detectable and the interaction between mouse GASP1 and human Beclin 2 was barely detectable (Figures 3B-C). The interaction is specific for GASP1 and not other related family members, as GASP2 did not co-immunoprecipitate with Beclin 2 (Figure 5A). We also confirmed that endogenous GASP1 interacts with endogenous Beclin 2 but not endogenous Beclin 1 in co-immunoprecipitation experiments in HEK293 cells (Figure 3D and Figure S3). Consistent with the yeast two-hybrid screen results, Beclin 2 coimmunoprecipitated with a C-terminal fragment (amino acids 899-1395) of GASP1 (Figure 3E). Taken together, these data demonstrate that GASP1 is a unique interaction partner of Beclin 2, but not of Beclin 1, and that this interaction is mediated through the N-terminal region of Beclin 2 and the C-terminal region of GASP1.

Beclin 2 is Required for the Endolysosomal Trafficking and Degradation of GPCRs

As Beclin 2, but not Beclin 1, interacts with GASP1, we hypothesized that Beclin 2 may selectively function in the endolysosomal trafficking and degradation of GPCRs that are regulated by their C terminal interactions with GASP1. To test this hypothesis, we used the biotin protection degradation assay (Whistler et al., 2002) to measure the degradation of GPCRs that are degraded by post-endosomal sorting to the lysosome (Figure S4A) in the presence of different autophagy gene siRNAs or cGASP overexpression (Figure S4B).

First, we used the DOR as a marker substrate (Figure 4A, 4B). In HEK293 cells that stably express Flag-DOR, after 30 min of DADLE ([D-Ala^2, D-Leu^5]-Enkephalin) agonist treatment, the biotinylated receptors are internalized and protected from membrane stripping, and can be detected by the presence of biotin signal in cell lysates immunoprecipitated by anti-Flag antibody. After longer agonist treatment (180 min), the endocytosed receptors are transported to the lysosome, where they are degraded; thus, the levels of detectable biotinylated receptors after membrane stripping are minimal. This receptor degradation is dependent on lysosomal function, as it is blocked in cells treated with the lysosomal inhibitor, bafilomycin A1 (Figure S4C). The pattern of lysosomal degradation of biotinylated DOR was similar in cells treated with non-silencing control siRNA as in cells treated with *beclin 1* siRNA, *ATG14* siRNA, and *VPS34* siRNA, indicating that the Beclin 1/VPS34/ATG14 complex (which is involved in autophagy) is not involved in GPCR degradation. In contrast, *beclin 2* siRNA treatment resulted in the retention of biotinylated intracellular DOR after prolonged agonist treatment (180 min), suggesting that Beclin 2 is required for the endolysosomal trafficking and degradation of certain GPCRs. This block in DOR degradation with *beclin 2* siRNA treatment is similar to that observed with overexpression of C-terminal GASP1, a dominant negative form of GASP1 (Whistler et al., 2002). In addition to DOR, we found that degradation of two other GASP1-associated GPCRs, CB1R (Figure 4C) and β-Ala (Figure 4D), were dependent on Beclin 2. *Beclin 2* siRNA, but not *beclin 1* siRNA, increased levels of biotin-protected internalized CB1R and β-Ala receptors at 180 min as robustly as cGASP1 overexpression.

We confirmed the role of Beclin 2 in the post-endosomal sorting of DOR to the lysosome by fluorescent microscopy (Figure 4E). By pulse-labeling cell surface DOR with antibody, we found that *beclin 2*, but not *beclin 1*, siRNA treatment resulted in the trapping of internalized DORs in EEA1-positive endosomal structures and their failure to be transported to LAMP1-positive lysosomes after 60 min of agonist treatment.

Together, our results indicate that Beclin 2 is essential for agonist-induced lysosomal turnover of several GASP1-interacting GPCRs, including the DOR, CB1R, and β-Ala receptor, and that Beclin 2 and Beclin 1 do not functionally overlap in GPCR degradation. Moreover, the role of Beclin 2 in endolysosomal trafficking may be limited to GASP1-dependent GPCRs; *beclin 2* siRNA had no effect on agonist-induced lysosomal degradation of another GPCR that is not regulated by GASP1, the chemokine receptor, CXCR4, or a receptor tyrosine kinase, PDGFR (Figures S4D-F).

The signaling function of many GPCRs is regulated by post-endosomal sorting to lysosomes and degradation (Hanyaloglu and von Zastrow, 2008). After agonist withdrawal and/or

antagonist treatment, some types of internalized GPCRs are recycled back to the plasma membrane and re-sensitized, while others are sorted to lysosomes for degradation and signaling down-regulation, such as several GASP1-associated GPCRs. To test whether loss of Beclin 2 leads to the recycling and re-sensitization of GPCRs, we analyzed antagonist-induced receptor recycling after *beclin 2* siRNA treatment. Using either the biotin protection degradation assay or pulse-chase experiments of antibodylabeled cell surface DOR detected by fluorescent microscopy, we found that the agonist-induced internalized DOR in *beclin 2* siRNA-treated cells recycled to the cell surface within 30 min after antagonist treatment (Figure 4F, 4G). Thus, the absence of Beclin 2-dependent lysosomal degradation of internalized GPCR allows their recycling back to the plasma membrane.

The Beclin 2-GASP1 Interaction Is Required for GPCR Degradation But Not for Autophagy

As Beclin 2 interacts with GASP1 and is required for the degradation of GASP1-dependent GPCRs, we hypothesized that it may function in GPCR degradation through a mechanism involving its interaction with GASP1. To evaluate this hypothesis, we sought to identify a single amino acid mutation in Beclin 2 that blocks binding to GASP1. First, we tested whether amino acids 69-88 (predicted to be important based on secondary structure) of Beclin 2 were required for GASP1 binding, and found that GASP1 failed to co-immunoprecipitate with a mutant of Beclin 2 lacking these amino acids (Figure 5A). Next, to identify point mutations within this region that might block GASP1 binding to Beclin 2, we made substitution mutations within amino acids 69-88, focusing on residues that are conserved in orthologs of Beclin 2 (which binds to GASP1) but not in orthologs of Beclin 1 (which does not bind to GASP1) (Figure 5B). An isoleucine to serine mutation at amino acid 80 (Beclin 2 I80S) blocked GASP1 co-immunoprecipitation with Beclin 2 (Figure 5C), whereas substitutions at neighboring positions (D70R, K75A, and H77A) had no effect on the Beclin 2/GASP1 interaction. Thus, I80 is essential for the Beclin 2-GASP1 interaction, and the replacement of Beclin 2 isoleucine with a serine located in the identical position in Beclin 1 disrupts the Beclin 2-GASP1 interaction.

We used the Beclin 2 I80S mutant to investigate whether the Beclin 2-GASP1 interaction is necessary for Beclin 2 to function in GPCR degradation and in autophagy. We analyzed DOR degradation using the biotin protection assay in HEK293 cells transfected with *beclin 2* siRNA and three different *beclin 2* siRNA-resistant rescue plasmids that restore Beclin 2 expression in *beclin 2* knockdown cells (Figure 5D) including one encoding wild-type Beclin 2, one encoding Beclin 2 I80S, and one encoding Beclin 2Δ69-88. The wild-type Beclin 2 rescue plasmid reversed the effect of *beclin 2* knockdown on GPCR degradation, whereas the non-GASP1-interacting Beclin 2 I80S and Beclin 2Δ69-88 rescue plasmids had no effect (Figure 5E-F). In contrast, both wild-type Beclin 2 as well as non-GASP1-interacting mutants of Beclin 2 (Beclin 2 I80S and Beclin 2Δ69-88) rescued starvation-induced autophagy in *beclin 2* knockdown HeLa cells (Figure 5G-H). In addition, overexpression of the dominant negative C-terminal GASP1 did not block starvation-induced autophagy (Figure S5). Our results indicate that GASP1 and the Beclin 2-GASP1 interaction are essential for agonist-induced GPCR degradation, but are dispensable for autophagy, and that autophagy and GPCR degradation are two separate pathways that converge on Beclin 2.

Deficiencies in Autophagy and GPCR Degradation in *beclin 2* Knockout Mice

To study the *in vivo* functions of Beclin 2, we generated targeted mutant mice with a null mutation in *beclin 2* (Figures S6A, S6B). Embryonic and postnatal survival rates of *beclin 2* homozygous knockout mice were markedly lower than predicted by Mendelian ratios (∼4% (4/117)) (Figure 6A). We confirmed the loss of Beclin 2 protein expression in MEFs and brain tissues of *beclin 2* knockout mice (Figures 6B and S6C). In primary MEFs derived from *beclin* $2^{+/+}$, *beclin* $2^{+/-}$ and *beclin* $2^{-/-}$ littermates (Figure 6B), there was less starvation-induced decrease in p62 degradation, decreased ratios of LC3-II to LC3-I in basal and starvation conditions, and increased levels of total LC3 in basal and starvation conditions in *beclin 2*-deficient MEFs compared with wild-type controls (Figure 6C, S6D). By quantitative electron microscopic analysis, no genotype-specific differences in basal autophagy were detected (although a trend towards decreased autophagy was observed in *beclin* $2^{-/-}$ MEFs) (Figure 6D and 6E). During starvation, both *beclin* $2^{+/-}$ and *beclin* $2^{-/-}$ MEFs had fewer autophagic structures (autophagosomes and autolysosomes) than wild-type *beclin* $2^{+/+}$ MEFs. *Beclin* $2^{-/-}$ MEFs, but not *beclin* $2^{+/-}$MEFs, showed a decrease in long-lived protein degradation during basal conditions as compared to *beclin* $2^{+/+}$ MEFs, whereas long-lived protein degradation was decreased during starvation conditions in both *beclin* $2^{+/-}$ and *beclin* $2^{-/-}$ MEFs (Figure 6F). (The magnitude of this decrease was small; biallelic deletion of *beclin 2* had a similar, not greater, effect than monoallelic deletion of *beclin 1* (Figure S6E).) In addition, the brains of *beclin* $2^{+/-}$ mice had elevated levels of total LC3, decreased conversion of LC3-I to LC3-II, and increased p62 accumulation as compared with those of wild-type littermates (Figure S6F). Together, these data suggest that *beclin 2* gene deletion impairs, but does not completely abrogate, basal and starvation-induced autophagy.

Of note, we observed higher steady-state levels of CB1R in *beclin* $2^{+/-}$ and *beclin* $2^{-/-}$MEFs than in wild-type controls (Figure 6G). We also detected higher levels of CB1R expression in brain lysates of *beclin* $2^{+/-}$ mice as compared to wild-type *beclin* $2^{+/+}$ littermates (Figure 6H). In contrast, no increase in CB1R expression was detected in the brains of *beclin* $1^{+/-}$ mice as compared to their wild-type littermates, suggesting this increase was not due to a defect in Beclin family member-dependent autophagy. Rather, these data are consistent with our siRNA knockdown data in cultured cells indicating that Beclin 2, but not Beclin 1, is involved in GASP1-dependent GPCR degradation. In further support of this conclusion, the brains of *beclin* $2^{+/-}$ mice had increased levels of the dopamine 2 receptor (another GPCR regulated by GASP1), but no difference in levels of the mu opioid receptor, which does not bind GASP1 (Figure S6G).

Thus, our data in *beclin* $2^{-/-}$ MEFs and *beclin* $2^{+/-}$ mice demonstrate that Beclin 2 functions in two distinct lysosomal degradation pathways, autophagy and the endolysomal trafficking and degradation of certain GPCRs.

beclin 2 Heterozygous Knockout Mice Develop Obesity and Insulin Resistance

In mice, excess CB1R signaling increases food intake, results in weight gain and promotes diabetes/insulin resistance (Maccarrone et al., 2010), whereas pharmacological antagonism of CB1R or genetic deletion of CB1R has the opposite effects on food intake, weight and insulin resistance (Di Marzo, 2008). Therefore, we sought to examine whether *beclin 2*

heterozygous mice develop obesity and/or insulin resistance. We fed 8 week-old *beclin 2*$^{+/-}$ mice or wild-type littermates either regular diet (RD) or high-fat diet (HFD) for 8 weeks and measured body weight, food intake and insulin sensitivity. *beclin 2*$^{+/-}$ mice gained more weight (Figure 7A) and had more food intake (Figure 7B) than wild-type mice in either condition, despite comparable spontaneous physical activity (Figures S7A and S7B), suggesting that their increased body weight is likely caused by increased energy intake rather than decreased energy expenditure. Furthermore, compared to wild-type littermates, *beclin 2*$^{+/-}$ mice demonstrated impaired glucose tolerance (Figure 7C and 7D, left graphs) and decreased insulin sensitivity (Figure 7C and 7D, right graphs) in RD and HFD conditions (see also Figure S7C-E). None of these differences were observed in mice with monoallelic loss of *beclin 1* (Figure S7F-I). Thus, *beclin 2* exerts a unique role in metabolic regulation that is not shared by *beclin 1*.

To investigate whether CB1R accumulation contributes to the diabetic phenotype in *beclin 2*$^{+/-}$ mice, we evaluated the effects of treatment with the CB1R antagonist rimonabant (Di Marzo, 2008) on glucose tolerance in mice fed a regular diet. As predicted, body weight decreased in both wild-type and *beclin 2*$^{+/-}$ mice in response to rimonanbant given for two weeks (Figure 7E). However, rimonabant did not affect glucose tolerance curves in wild-type mice, but decreased the glucose intolerance observed in *beclin 2*$^{+/-}$ mice (Figure 7F, Figure S7J). This suggests that glucose intolerance in *beclin 2*$^{+/-}$ mice may be partly caused by a failure in CB1R downregulation. Taken together, our data in *beclin 2*$^{+/-}$ mice are consistent with a role of Beclin 2-dependent degradation of CB1R in glucose homeostasis.

Discussion

Our results demonstrate that Beclin 2 is a novel Atg6/Beclin family member that functions in two different lysosomal degradation pathways that are essential for cellular homeostasis, autophagy and the downregulation of certain seven transmembrane-spanning GPCRs. The function of Beclin 2 in agonist-induced GPCR lysosomal degradation is genetically distinct from that in autophagy. It does not involve Beclin 1 or other Beclin 1/2-interacting proteins such as ATG14 and VPS34 that function in autophagy. In addition, starvation-induced autophagy, but not agonist-induced GPCR degradation, can be rescued in *beclin 2* knockdown cells by a Beclin 2 mutant that cannot interact with GASP1. The function of Beclin 2 in agonist-induced lysosomal degradation is also likely distinct from other autophagy-independent trafficking functions previously described for yeast Atg6/Vps30 or mammalian Beclin 1, such as vacuolar protein sorting and EGFR degradation (Funderburk et al., 2010). These functions involve the Atg6/Beclin 1-interacting class III PI3K, VPS34, whereas we did not observe a role for human VPS34 in the degradation of GASP1-dependent GPCRs. Thus, Beclin 2 exerts an autophagy-independent and class III PI3K-independent function in the endolysosomal trafficking and degradation of GASP1-regulated GPCRs.

The dual, but mechanistically non-overlapping, functions of Beclin 2 in autophagy and GPCR degradation raise many questions. In terms of autophagy, it is unclear why a second “Beclin” is needed. The intronless nature of human Beclin 2, differential pattern of tissue expression, and differential interaction pattern of Beclin 2 versus Beclin 1 with certain

autophagy regulatory proteins (e.g. Bcl-2, AMBRA1, and Rubicon) may underlie as-of-yet undefined unique regulatory or functional features of Beclin 2 in autophagy. Perhaps differential mRNA stability or different kinetics of gene expression of intronless human Beclin 2 versus human Beclin 1 (which has multiple introns) contributes to temporal and/or spatial differences in its functions in autophagy induction in response to different stimuli and in different cell types or tissues. Similarly, the restricted tissue pattern of expression of Beclin 2 versus Beclin 1 (which is expressed ubiquitously) may reflect different roles of different Beclin family members in autophagy regulation in different tissues. The binding patterns of Beclin 2 suggest that, unlike Beclin 1, it may not need to be “unleashed” from negative regulators; during basal conditions in HeLa cells, we could not detect any binding of Beclin 2 to the negative regulator, Rubicon, and we detected a marked increase in binding to the positive regulator, AMBRA1. Moreover, unlike with Beclin 1, starvation-induced autophagy does not appear to require disruption of the Bcl-2/Beclin 2 complex; we speculate that this may be due to lack of conservation in Beclin 2 of the T119 site in Beclin 1 that is phosphorylated by DAPK to promote disruption of Beclin 1 from binding to Bcl-2/Bcl-x_L (Zalckvar et al., 2009). Furthermore, given the findings that Bcl-2 sequesters AMBRA1 away from Beclin 1 (Strappazzon et al., 2011), the basal increase in AMBRA1 interaction with Beclin 2 may bypass the need for Bcl-2/Bcl-x_L to dissociate from Beclin 2 during autophagy induction. Future studies addressing the molecular regulation of Beclin 2 may unravel previously unappreciated levels of complexity in the regulation of Atg6/Beclin family members in autophagy.

Although mechanistically distinct, the dual functions of Beclin 2 in GPCR degradation and autophagy may result in hitherto unknown cross-talk between the two pathways. It is possible that agonists of GASP1-dependent GPCRs (which trigger their endolysosomal trafficking and degradation) “divert” Beclin 2 from an autophagy pathway to a GPCR degradation pathway. Conversely, it is possible that GPCR agonists might upregulate Beclin 2 expression, providing a larger pool of Beclin 2 to act in autophagy. It is noteworthy that cannabinoids, agonists of the CB1R, and morphine, an opioid receptor agonist, induce autophagy (Salazar et al., 2009; Zhao et al., 2010) Although a variety of mechanisms for these actions of cannabinoid and opiate-induced autophagy have been proposed, including activation of ER stress, ROS generation, and the upregulation of Beclin 1 expression, the precise mechanisms by which CB1R and DOR agonists induce autophagy are not completely understood. Beclin 2, which functions in agonist-induced degradation of CB1Rs and DORs, may also function in GPCR agonist-induced autophagy regulation.

More broadly, the dual function of Beclin 2 in mammalian GPCR degradation and autophagy may reflect a need for higher eukaryotes to tightly coordinate these different facets of the cellular response to environmental cues. Interestingly, the majority of mammalian GPCRs are expressed in the brain and modulate neuronal function (Gainetdinov et al., 2004), and Beclin 2 has high expression in mouse and human brain (Figure 1B and data not shown). In addition, although the DOR, CB1R, and β-adrenergic receptor have exons, the majority of mammalian GPCRs are intronless, and GPCRs constitute the majority of mammalian intronless genes (Gentles and Karlin, 1999). The evolutionary basis for the selection of this gene structure for mammalian GPCRs remains unclear, but similar factors may have resulted in the co-evolution of human Beclin 2 (a protein involved in GPCR

regulation) which is also intronless. Aside from this parallelism in the evolution of mammalian GPCR gene structure and human Beclin 2 gene structure, the use of an Atg6/Beclin autophagy gene homolog in the endolyososomal trafficking and degradation of CNS-expressed GPCRs suggests an evolutionary advantage to coupling two distinct trafficking functions (endolysosomal degradation of GPCRs and autophagy) in the same protein.

Our discovery of a role for Beclin 2 in the degradation of GASP1-regulated GPCRs represents a mechanistic advance in understanding agonist-induced GPCR degradation. GASP1, originally identified in a yeast two-hybrid screen with the C terminus of the DOR (Whistler et al., 2002), is expressed predominantly in the CNS (similar to Beclin 2) (Abu-Helo and Simonin, 2010; Simonin et al., 2004) and modulates the postendocytic sorting of a highly specific subset of GPCRs to the lysosome for degradation in a ubiquitin-independent manner (Moser et al., 2010). This targeting of GPCRs to the degradative/lysosomal pathway has been shown to regulate virally-encoded GPCR signaling *in vitro* (Tschische et al., 2010), and manipulation of GASP1 function *in vivo* regulates pharmacological responses to cannabinoids (agonists of CB1R) and cocaine (an indirect agonist of the dopamine D2 receptor) (Moser et al., 2010). Thus, GASP1-dependent sorting likely plays a key physiological role in the regulation of signaling pathways mediated by GASP1-interacting GPCRs. However, aside from its well-described high affinity interactions with cytoplasmic tails of multiple GPCRs (Heydorn et al., 2004), little is known about the molecular mechanisms of GASP1 function, including its site of action in the endocytic pathway and the identity of sorting machinery or other proteins with which it may interact. The discovery of Beclin 2 as a novel GASP1 binding partner provides new insights into the mechanisms by which GASP1-regulated GPCRs are fated for endolysosomal degradation.

We speculate that the function of Beclin 2 in GPCR degradation, like GASP1, may be important in regulating cannabinoid receptor signaling. Amongst the three types of known cannabinoid receptors found in mammals (CB1R, CB2R, CB3R) (Maccarrone et al., 2010), CB1R is the major receptor in the brain involved in the regulation of food intake and energy balance. It can be induced by the exogenous administration of cannabinoids, which are the active ingredient of *Cannabis sativa*, as well as by endocannabinoids, a family of polyunsaturated lipids endogenously synthesized as natural ligands of the CB1R. CB1R activation by these exogenous or endogenous agonists leads to increased appetite, increased food intake, and an obesity/diabetes phenotype (Maccarrone et al., 2010), whereas CB1R knockout mice are lean with reduced food intake (Cota et al., 2003). Moreover, CB1R antagonists, such as rimonabant, reduce body weight and insulin resistance in both obese rodents and humans (Di Marzo, 2008). In our study, we noted that *beclin 2* heterozygous-deficient mice have elevated levels of brain CB1R expression, increased body weight, increased food intake, and insulin resistance. These phenotypes are highly consistent with increased CB1R signaling; yet, we cannot definitively conclude that there is a causal relationship between the elevated levels of CNS CB1R expression and the physiological abnormalities we noted in the *beclin 2* heterozygous-deficient mice, as other functions of *beclin 2* may contribute to these abnormalities. However, it is unlikely they are related to decreased autophagy, as we found that *beclin 1* heterozygous-deficient mice did not have increased CNS expression of CB1R, increased body weight, increased food intake or insulin

resistance. Further investigations are warranted to investigate whether mouse *beclin 2* allelic loss alters other GASP1-dependent GPCR signaling functions *in vivo*.

Interestingly, chromosome 1q43, the genetic locus that contains human *beclin 2*, has been linked to obesity and diabetes-related traits in multiple ethnic populations, including Caucasians, Mexican Americans, Pacific Islanders and Caribbean Hispanics (Aissani et al., 2006; Bosse et al., 2004; Dong et al., 2011; Schelling et al., 2008; Shmulewitz et al., 2006). Additional genetic studies are needed to determine whether *beclin 2* is a bona fide risk allele for obesity and diabetes in humans. Our findings that *beclin 2* heterozygous-deficient mice have increased body weight and insulin resistance provide a strong rationale for such studies; Beclin 2 may represent a newly identified regulator of body weight and glucose homeostasis not only in mice, but also in humans.

Experimental Procedures

Cell Culture

HEK293 cell lines stably expressing Flag epitope-tagged GPCRs have been previously described (Martini et al., 2007; Whistler et al., 2002). Primary MEFs were isolated from offspring at day e13.5 of autophagy mutant mice (described in Extended Experimental Procedures). HEK293, HeLa, mouse Neuro2A and CCD-1064Sk cell lines were obtained from ATCC (American Type Culture Collection). HeLa/GFP-LC3 cells were previously described (Orvedahl et al., 2010).

Yeast Two-Hybrid Screen

The yeast two-hybrid screen of human Beclin 2 N-terminal region (amino acids 1-88) binding partners was performed using the Matchmaker™ Gold Yeast Two-Hybrid System (Clontech). The bait *GAL4* Beclin 2-BD fusion was cloned into pGBKT7, and transformed into the yeast strain Y187 containing the Mate & Plate™ Library of human brain cDNAs (Clontech), according to the manufacturer's instructions.

Co-immunoprecipitation

Cells were lysed in lysis buffer and subjected to immunoprecipitation with anti-Flag antibody, anti-Myc antibody, anti-Beclin 2 antibody or anti-Beclin 1 antibody. Eluates were separated by SDS-PAGE and detected by western blot analyses. For details of conditions and antibodies used, see Extended Experimental Procedures.

Biotin Protection Degradation Assay

The biotin protection degradation assay was performed on HEK293 cells stably expressing Flag epitope-tagged receptors using a modification of the method previously described (Whistler et al, 2002). See Extended Experimental Procedures for details.

Receptor Internalization and Recycling Assay

The antibody-feeding immunofluorescence DOR recycling assay was performed as described in detail in Extended Experimental Procedures using 140 min agonist (5 μM DADLE) and 30 min antagonist (10 μM naloxone) treatment.

Autophagy Assays

Autophagy was measured by LC3 and p62 western blotting, quantitative electron microscopy, measurement of long-lived protein degradation, and quantitation of GFP-LC3 puncta in HeLa/GFP-LC3 cells. For details, see Extended Experimental Procedures.

Contruction of *beclin 2* Knockout Mice

The targeting construct with the *beclin 2* coding region replaced by a neomycin marker flanked by LoxP sites was electroporated into ES cells. The knockout clones were screened and injected into donor blastocysts, and offspring with germline transmission were bred to mice expressing Cre from the CAG promoter to remove the neomycin cassette. For detailed methods, see Extended Experimental Procedures.

Animal Experiments

Male C57BL/6J mice (*beclin* $2^{+/-}$, *beclin* $1^{+/-}$ and wild-type littermates) were housed on a 12-h light/dark cycle. They were fed either with a RD (Harlan Teklad) or a HFD containing 60% fat (Research Diets, D12492). Rimonabant (Cayman Chemical) was administered intraperitoneally (i.p.) in phosphate buffered saline (PBS) with 0.3% Tween 80 (10 mg kg^{-1} body weight daily). All animal protocols were approved by the UTSW Medical Center Institutional Animal Care and Use Committee.

Mouse Metabolic Studies and Blood Tests

Food intake and physical activity were measured in TSE metabolic chambers (TSE Systems) over a five day-period. Glucose tolerance tests were performed by i.p. glucose injection (1 g kg^{-1}) after a 3 h fast. Insulin tolerance tests were performed by i.p. insulin (Novo Nordisk and Sigma) injection (0.8 unit kg^{-1}) after a 3 h fast. Blood was drawn from tail veins at the indicated time points after glucose or insulin injection, and serum glucose levels were analyzed using commercial glucose assay reagents (Sigma, Cat# 6918, P7119, F5803).

Statistical Analyses

For comparisons of the means of two groups, one-way ANOVA was used. For comparison of multiple groups with a control group, ANOVA with the Dunnet method was used. Linear mixed effect models (which compares differences between groups, while accounting for correlations within the same subject) were used to compare different changes for slopes of linear curves among groups. To determine the difference between non-linear curves in two groups, analyses were performed using the statistical modeling package, *statmod*, which is available from the R Project for Statistical Computing (http://www.r-project.org).

Supplementary Material

Refer to Web version on PubMed Central for supplementary material.

Acknowledgments

We thank Haley Harrington for assistance with manuscript preparation, and the Electron Microscopy Unit of the Institute of Biotechnology, University of Helsinki, Finland for providing laboratory facilities. This work was supported by NIH awards, ROI CA109618 (B.L.), ROI GM094575 (N.V.G), ROI DK55758 (P.E.S), PO1

DK088761 (P.E.S), ROI DA019958 (J.L.W), ROI DK043351 (R.X.), K99 DK094980 (C.H), R21 AI078198 (S.S.), P20 RR015566 (S.S); a Welch Foundation Award I-1505 (N.V.G); and funds provided by the state of California for medical research on alcohol and substance abuse through the University of California, San Francisco to J.L.W. E.-L.E. was supported by the Academy of Finland. The authors Yongjie Wei, Kai Sun, and Binghua Li all contributed equally to this manuscript.

References

Abu-Helo A, Simonin F. Identification and biological significance of G protein-coupled receptor associated sorting proteins (GASPs). Pharmacol Ther. 2010; 126:244–250. [PubMed: 20394773]

Aissani B, Perusse L, Lapointe G, Chagnon YC, Bouchard L, Walts B, Bouchard C. A quantitative trait locus for body fat on chromosome 1q43 in French Canadians: linkage and association studies. Obesity (Silver Spring). 2006; 14:1605–1615. [PubMed: 17030972]

Bosse Y, Chagnon YC, Despres JP, Rice T, Rao DC, Bouchard C, Perusse L, Vohl MC. Genome-wide linkage scan reveals multiple susceptibility loci influencing lipid and lipoprotein levels in the Quebec Family Study. J Lipid Res. 2004; 45:419–426. [PubMed: 14679165]

Chen Y, Klionsky DJ. The regulation of autophagy - unanswered questions. J Cell Sci. 2011; 124:161–170. [PubMed: 21187343]

Cota D, Marsicano G, Tschop M, Grubler Y, Flachskamm C, Schubert M, Auer D, Yassouridis A, Thone-Reineke C, Ortmann S, et al. The endogenous cannabinoid system affects energy balance via central orexigenic drive and peripheral lipogenesis. J Clin Invest. 2003; 112:423–431. [PubMed: 12897210]

Di Marzo V. CB(1) receptor antagonism: biological basis for metabolic effects. Drug Discov Today. 2008; 13:1026–1041. [PubMed: 18824122]

Dong C, Beecham A, Slifer S, Wang L, McClendon MS, Blanton SH, Rundek T, Sacco RL. Genome-wide linkage and peak-wide association study of obesity-related quantitative traits in Caribbean Hispanics. Hum Genet. 2011; 129:209–219. [PubMed: 21104097]

Funderburk SF, Wang QJ, Yue Z. The Beclin 1-VPS34 complex--at the crossroads of autophagy and beyond. Trends Cell Biol. 2010; 20:355–362. [PubMed: 20356743]

Gainetdinov RR, Premont RT, Bohn LM, Lefkowitz RJ, Caron MG. Desensitization of G protein-coupled receptors and neuronal functions. Annu Rev Neurosci. 2004; 27:107–144. [PubMed: 15217328]

Gentles AJ, Karlin S. Why are human G-protein-coupled receptors predominantly intronless? Trends Genet. 1999; 15:47–49. [PubMed: 10098406]

Hanyaloglu AC, von Zastrow M. Regulation of GPCRs by endocytic membrane trafficking and its potential implications. Annu Rev Pharmacol Toxicol. 2008; 48:537–568. [PubMed: 18184106]

Heydorn A, Sondergaard BP, Ersboll B, Holst B, Nielsen FC, Haft CR, Whistler J, Schwartz TW. A library of 7TM receptor C-terminal tails. Interactions with the proposed post-endocytic sorting proteins ERM-binding phosphoprotein 50 (EBP50), N-ethylmaleimide-sensitive factor (NSF), sorting nexin 1 (SNX1), and G protein-coupled receptor-associated sorting protein (GASP). J Biol Chem. 2004; 279:54291–54303. [PubMed: 15452121]

Hurley JH, Emr SD. The ESCRT complexes: structure and mechanism of a membrane-trafficking network. Annu Rev Biophys Biomol Struct. 2006; 35:277–298. [PubMed: 16689637]

Levine B, Mizushima N, Virgin HW. Autophagy in immunity and inflammation. Nature. 2011; 469:323–335. [PubMed: 21248839]

Maccarrone M, Gasperi V, Catani MV, Diep TA, Dainese E, Hansen HS, Avigliano L. The endocannabinoid system and its relevance for nutrition. Annu Rev Nutr. 2010; 30:423–440. [PubMed: 20645854]

Martini L, Waldhoer M, Pusch M, Kharazia V, Fong J, Lee JH, Freissmuth C, Whistler JL. Ligand-induced down-regulation of the cannabinoid 1 receptor is mediated by the G-protein-coupled receptor-associated sorting protein GASP1. FASEB J. 2007; 21:802–811. [PubMed: 17197383]

Mizushima N, Komatsu M. Autophagy: renovation of cells and tissues. Cell. 2011; 147:728–741. [PubMed: 22078875]

Mizushima N, Yoshimori T, Levine B. Methods in mammalian autophagy research. Cell. 2010; 140:313–326. [PubMed: 20144757]

Moser E, Kargl J, Whistler JL, Waldhoer M, Tschische P. G protein-coupled receptor-associated sorting protein 1 regulates the postendocytic sorting of seven-transmembrane-spanning G protein-coupled receptors. Pharmacology. 2010; 86:22–29. [PubMed: 20693822]

Orvedahl A, MacPherson S, Sumpter R Jr, Talloczy Z, Zou Z, Levine B. Autophagy protects against Sindbis virus infection of the central nervous system. Cell Host Microbe. 2010; 7:115–127. [PubMed: 20159618]

Pattingre S, Tassa A, Qu X, Garuti R, Liang XH, Mizushima N, Packer M, Schneider MD, Levine B. Bcl-2 antiapoptotic proteins inhibit Beclin 1-dependent autophagy. Cell. 2005; 122:927–939. [PubMed: 16179260]

Salazar M, Carracedo A, Salanueva IJ, Hernandez-Tiedra S, Lorente M, Egia A, Vazquez P, Blazquez C, Torres S, Garcia S, et al. Cannabinoid action induces autophagy-mediated cell death through stimulation of ER stress in human glioma cells. J Clin Invest. 2009; 119:1359–1372. [PubMed: 19425170]

Schelling JR, Abboud HE, Nicholas SB, Pahl MV, Sedor JR, Adler SG, Arar NH, Bowden DW, Elston RC, Freedman BI, et al. Genome-wide scan for estimated glomerular filtration rate in multi-ethnic diabetic populations: the Family Investigation of Nephropathy and Diabetes (FIND). Diabetes. 2008; 57:235–243. [PubMed: 18003762]

Shmulewitz D, Heath SC, Blundell ML, Han Z, Sharma R, Salit J, Auerbach SB, Signorini S, Breslow JL, Stoffel M, et al. Linkage analysis of quantitative traits for obesity, diabetes, hypertension, and dyslipidemia on the island of Kosrae, Federated States of Micronesia. Proc Natl Acad Sci U S A. 2006; 103:3502–3509. [PubMed: 16537441]

Simonin F, Karcher P, Boeuf JJ, Matifas A, Kieffer BL. Identification of a novel family of G protein-coupled receptor associated sorting proteins. J Neurochem. 2004; 89:766–775. [PubMed: 15086532]

Strappazzon F, Vietri-Rudan M, Campello S, Nazio F, Florenzano F, Fimia GM, Piacentini M, Levine B, Cecconi F. Mitochondrial BCL-2 inhibits AMBRA1-induced autophagy. EMBO J. 2011; 30:1195–1208. [PubMed: 21358617]

Tappe-Theodor A, Agarwal N, Katona I, Rubino T, Martini L, Swiercz J, Mackie K, Monyer H, Parolaro D, Whistler J, et al. A molecular basis of analgesic tolerance to cannabinoids. J Neurosci. 2007; 27:4165–4177. [PubMed: 17428994]

Tschische P, Moser E, Thompson D, Vischer HF, Parzmair GP, Pommer V, Platzer W, Schwarzbraun T, Schaider H, Smit MJ, et al. The G-protein coupled receptor associated sorting protein GASP-1 regulates the signalling and trafficking of the viral chemokine receptor US28. Traffic. 2010; 11:660–674. [PubMed: 20102549]

Whistler JL, Enquist J, Marley A, Fong J, Gladher F, Tsuruda P, Murray SR, Von Zastrow M. Modulation of postendocytic sorting of G protein-coupled receptors. Science. 2002; 297:615–620. [PubMed: 12142540]

Zalckvar E, Berissi H, Mizrachy L, Idelchuk Y, Koren I, Eisenstein M, Sabanay H, Pinkas-Kramarski R, Kimchi A. DAP-kinase-mediated phosphorylation on the BH3 domain of beclin 1 promotes dissociation of beclin 1 from Bcl-XL and induction of autophagy. EMBO Rep. 2009; 10:285–292. [PubMed: 19180116]

Zhao L, Zhu Y, Wang D, Chen M, Gao P, Xiao W, Rao G, Wang X, Jin H, Xu L, et al. Morphine induces Beclin 1- and ATG5-dependent autophagy in human neuroblastoma SH-SY5Y cells and in the rat hippocampus. Autophagy. 2010; 6:386–394. [PubMed: 20190558]

Research Highlights

- *beclin* 2 is a newly described autophagy gene
- Beclin 2 functions in endolysosomal degradation of GPCRs by binding to GASP1
- The functions of Beclin 2 in autophagy and GPCR degradation are genetically distinct
- Monoallelic loss of *beclin 2* in mice results in metabolic dysregulation

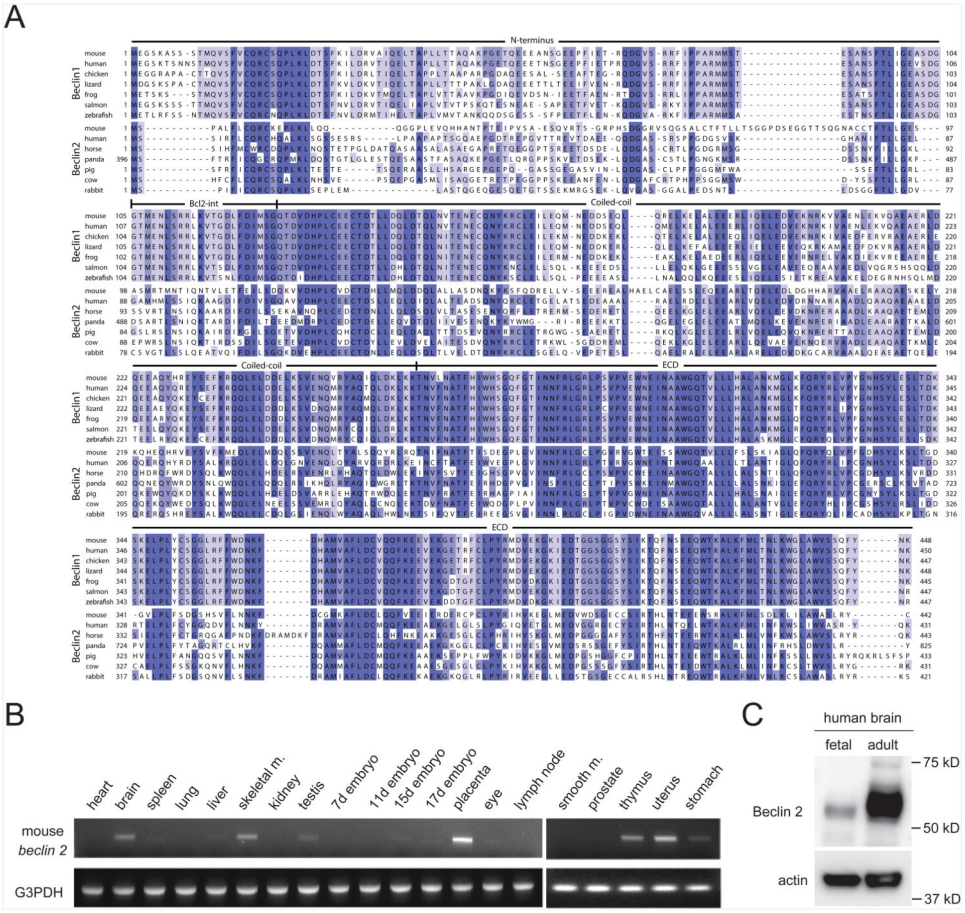

Figure 1. Sequence alignment and expression pattern of Beclin 2

(A) Alignment of Beclin 2 and Beclin 1 sequences. Shown are all known Beclin 2sequences, Beclin 1 sequences from selected mammalian organisms possessing Beclin 2,and Beclin 1 sequences from non-mammalian vertebrates whose genomes apparentlyencode only Beclin 1. See also Figure S1.

(B) RT-PCR analysis of mouse *beclin 2* expression level in different tissues using cDNA from a pool of approximately 200 mice.

(C) Western blot detection of human Beclin 2 in fetal and adult human brain lysates.

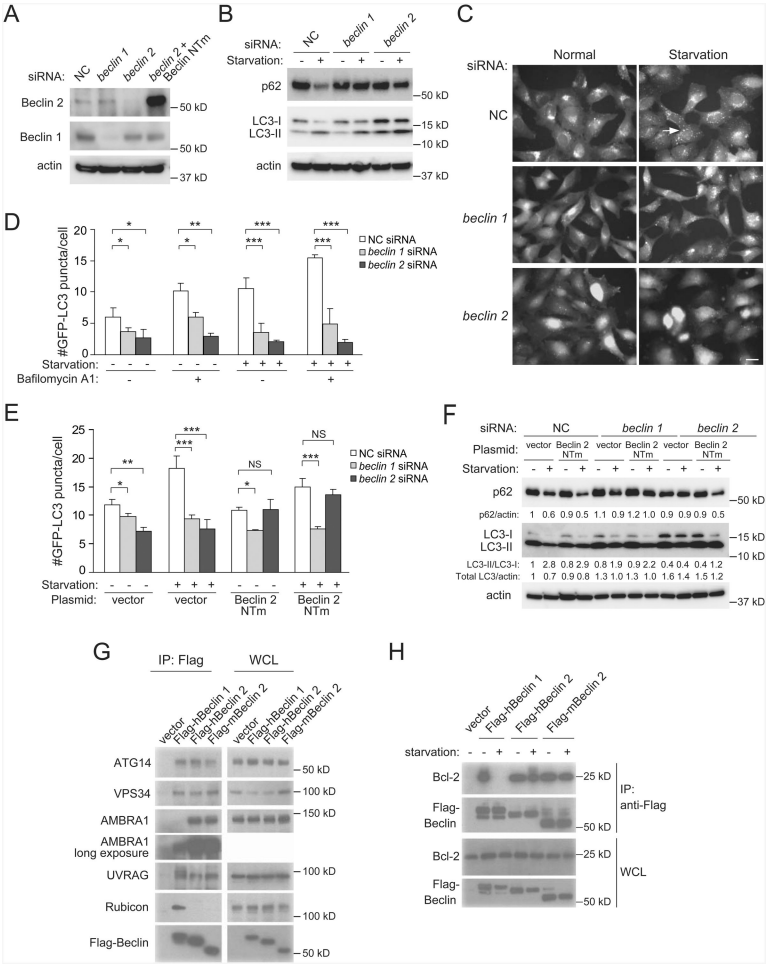

Figure 2. Beclin 2 functions in autophagy and interacts with known Beclin 1 binding partners

(A) Western blot detection of Beclin 1 and Beclin 2 in HeLa cells transfected with indicated siRNA. Beclin 2 NTm, an siRNA non-targetable mutant *beclin 2* rescue plasmid.

(B) Western blot detection of p62 and LC3 in HeLa cells transfected with indicated siRNA during growth in normal medium (starvation "−") or after 3 h amino acid and serum starvation (starvation "+"). See Figure S2B for quantitative analysis of western blots from three independent experiments.

(C) Representative images of GFP-LC3 puncta in HeLa/GFP-LC3 cells transfected with indicated siRNA and cultured for 3 h in normal or starvation medium. Arrow, representative autophagosome. Scale bar, 20 μm.

(D) Quantification of GFP-LC3 puncta in HeLa/GFP-LC3 cells transfected with indicated siRNA, treated with 100 nM bafilomycin A1 or vehicle (DMSO), and cultured for 3 h in normal or starvation medium.

(E) Quantification of GFP-LC3 puncta in HeLa/GFP-LC3 cells cotransfected with indicated siRNA and indicated plasmid, and cultured for 3 h in normal or starvation medium.

(F) Western blot detection of p62 in HeLa cells cotransfected with indicated siRNA andindicated plasmid, and cultured for 3 h in normal or starvation medium. Quantification

ofrelative levels of p62/actin, LC3-II/LC3-I and total LC3/actin is shown below each gellane.

(G) Co-immunoprecipitation of class III PI3K complex components with indicated Beclinproteins in HeLa cells transfected with indicated Flag-Beclin plasmids using an anti-Flagantibody.

(H) Co-immunoprecipitation of Bcl-2 with indicated Beclin proteins in HeLa cells transfected with indicated Flag-Beclin constructs using an anti-Flag antibody in nutrient-rich conditions or after 3 h of starvation.

For (D) and (E), bars represent mean represent mean ± SEM of triplicate samples (∼50 cells per sample) and similar results were observed in three independent experiments.

**P*<0.05; ***P*<0.01; ****P*<0.001; NS, not significant; ANOVA with Dunnett method.

NC, non-silencing control; WCL, whole cell lysate.

See also Figure S2.

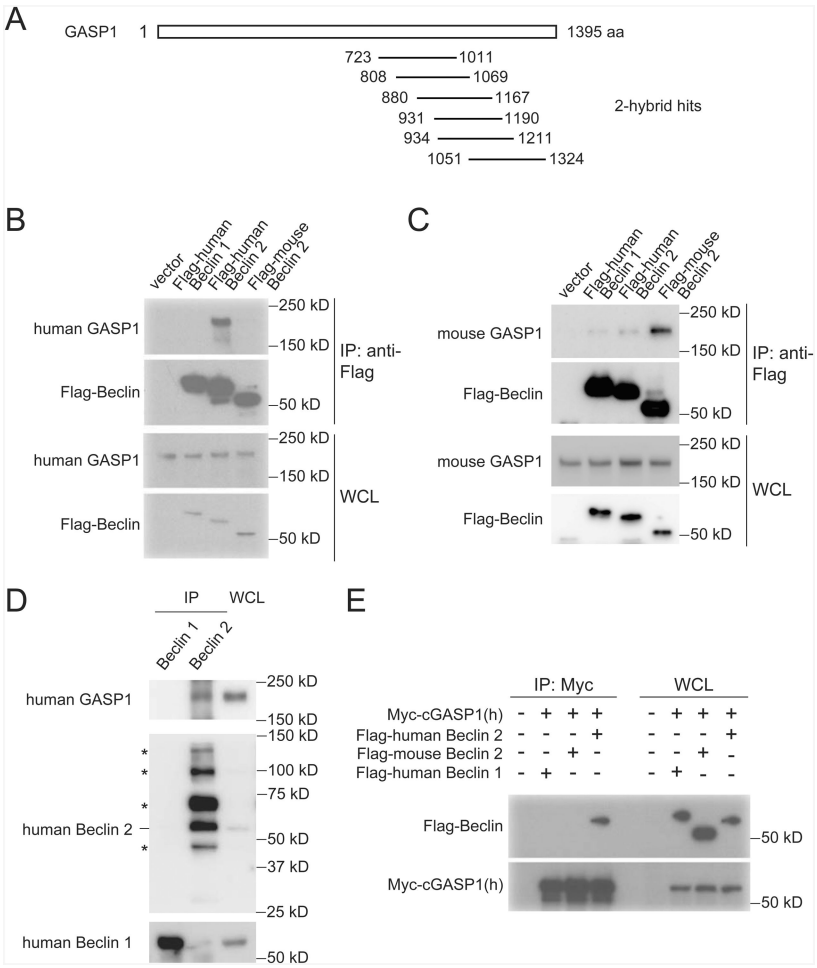

Figure 3. GASP1 is an interaction partner of Beclin 2

(A) Schematic depicting hits (14 colonies encoding proteins mapping to indicated amino acids of GASP1) isolated from yeast two-hybrid screen of human brain cDNA library using N-terminal human Beclin 2 (amino acids 1-88) as bait.

(B) Co-immunoprecipitation of endogenous human GASP1 with human Flag-Beclin 2 in HEK293 cells transfected with indicated plasmids.

(C) Co-immunoprecipitation of endogenous mouse GASP1 with mouse Flag-Beclin 2 in mouse Neuro2A cells transfected with indicated plasmids.

(D) Co-immunoprecipitation of endogenous GASP1 with endogenous Beclin 2 inHEK293 cells. Asterisks denote non-specific bands.

(E) Co-immunoprecipitation of Flag-human Beclin 2 with Myc-tagged C-terminal humanGASP1 in HeLa cells transfected with indicated plasmids.

cGASP1, C-terminal GASP1.

See also Figure S3.

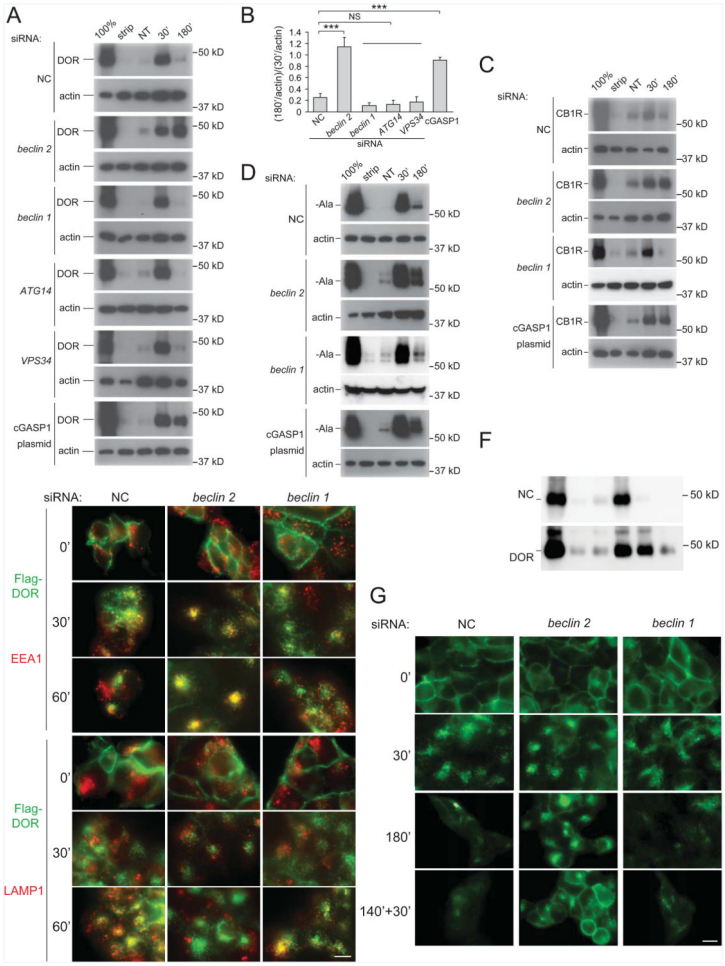

Figure 4. Beclin 2 is required for degradation of a subset of GPCRs

(A, C, D) Effects of indicated siRNA or cGASP1 overexpression on biotin-mediated protection of (A) the DOR after agonist treatment (DADLE, 5 μM) in HEK293 cells stably expressing Flag-DOR, (C) the CB1R after agonist treatment (WN 55,212-1 μM) in HEK293 cells stably expressing Flag-CB1R, and (D) the β-Ala receptor after agonist treatment (isoproterenol, 5 μM) in HEK293 cells stably expressing Flag-β-Ala. For (A, C, D), first lane (100%) represents total biotinylated GPCR prior to cell surface biotin stripping; second lane (strip) represents the remaining biotinylated GPCR after cell surface stripping; third lane (NT) represents the level of internalized biotinylated receptor with vehicle treatment after stripping; fourth and fifth lanes (30′, 180′) represent levels of internalized biotinylated receptor with agonist treatment for 30 min or 180 min, respectively, after stripping. Biotinylated Flag epitope-tagged GPCRs were precipitated with anti-Flag antibody, analyzed by SDS-PAGE, and detected with streptavidin overlay.

(B) Quantification of the ratio of DOR levels at 180 min versus 30 min in each condition shown in (A). Bars represent mean ± SEM of three independent experiments. ***P<0.001; NS, not significant; ANOVA with Dunnett method.

(E) Fluorescent microscopic imaging of DOR in HEK293 cells stably expressing Flag-DOR treated with indicated siRNAs. Cells were fed with anti-Flag antibody, treated with the agonist for 30 or 60 min, immunostained with anti-EEA1 or anti-LAMP1 primary

antibodies, and labeled with fluorescent secondary antibodies. Green, Flag-DOR; red, EEA1 or LAMP1. Scale bar, 10 μm.

(F) Effects of indicated siRNA on DOR recycling to the cell surface. HEK293/Flag-DORcells were treated with agonist for 30 min or 180 min as in (A), or in lane 6, treated withagonist for 140 min, antagonist for 30 min, and then subjected to stripping of cell surfacebiotin.

(G) Immunofluorescence analysis of effects of indicated siRNA on fate of cell surface-labeled Flag-DOR. HEK293/Flag-DOR were incubated with anti-Flag antibody, and then treated as in (F) (except without membrane stripping). Subcellular localization of Flag-DOR was detected by immunofluorescent staining. Scale bar, 10 μm.

See also Figure S4.

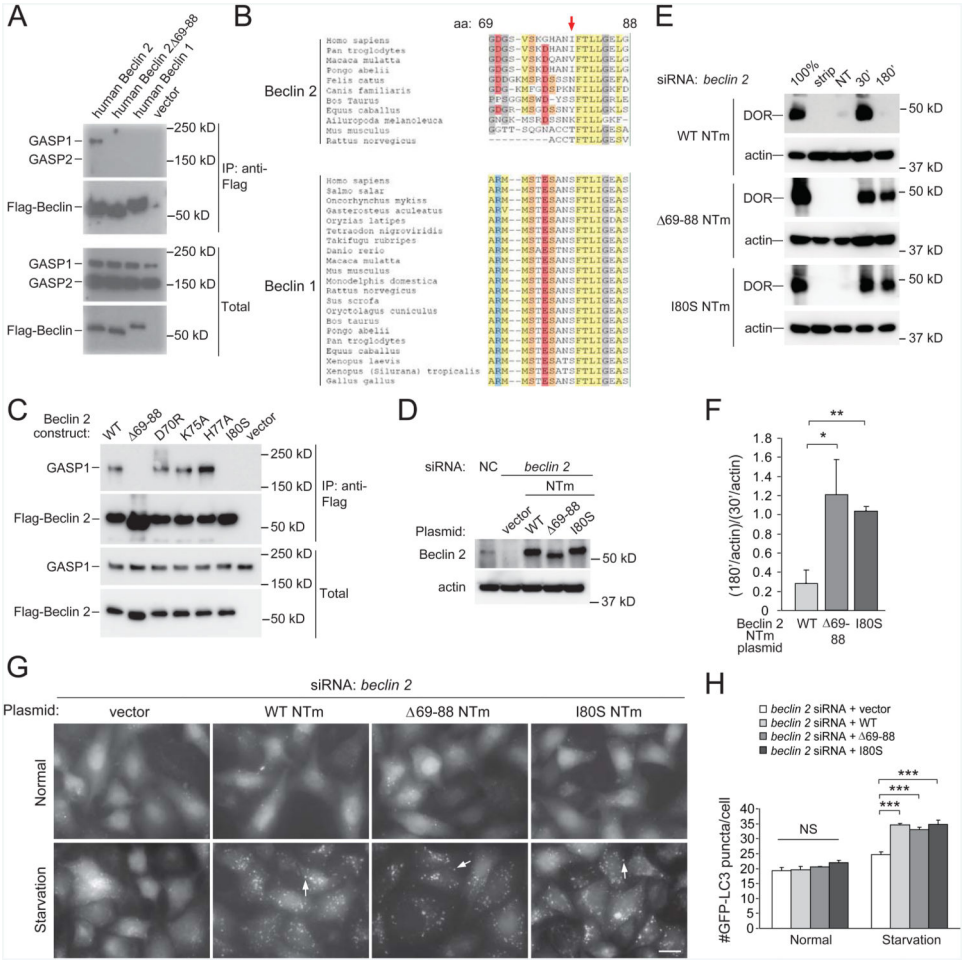

Figure 5. The Beclin 2-GASP1 interaction is essential for GPCR degradation but not autophagy

(A) Co-immunoprecipitation of endogenous GASP1 in HEK293 cells transfected with indicated Flag epitope-tagged Beclin constructs.

(B) Alignment of amino acids 69-88 of Beclin 2 and Beclin 1 family members. Red arrow denotes position of Beclin 2 I80 residue.

(C) Co-immnoprecipitation of endogenous GASP1 in HEK293 cells transfected with indicated Flag epitope-tagged wild-type (WT) or mutant Beclin 2 constructs.

(D) Expression of Beclin 2 in HEK293 cells co-transfected with *beclin 2* siRNA and indicated Beclin 2 NTm rescue plasmids.

(E) Effects of *beclin 2* siRNA and indicated plasmid co-transfection on biotin-mediatedprotection of the DOR after agonist treatment (DADLE, 5 μM) in HEK293/Flag-DORcells.

(F) Quantification of the ratio of DOR levels at 180 min versus 30 min in each conditionshown in (E). Bars represent mean ± SEM of three independent experiments.

(G) Representative images of GFP-LC3 puncta in HeLa/GFP-LC3 cells after co-transfection with *beclin 2* siRNA and indicated plasmid and culture for 3 h in normal or starvation medium. Arrows denote representative autophagosomes. Scale bar, 20 μm.

(H) Quantification of the GFP-LC3 puncta shown in (G). Bars represent mean ± SEM of triplicate samples (∼50 cells per sample). Similar results observed in three independent experiments.

*P<0.05; **P<0.01; ***P<0.001; NS, not significant; ANOVA with Dunnett method.

See also Figure S5.

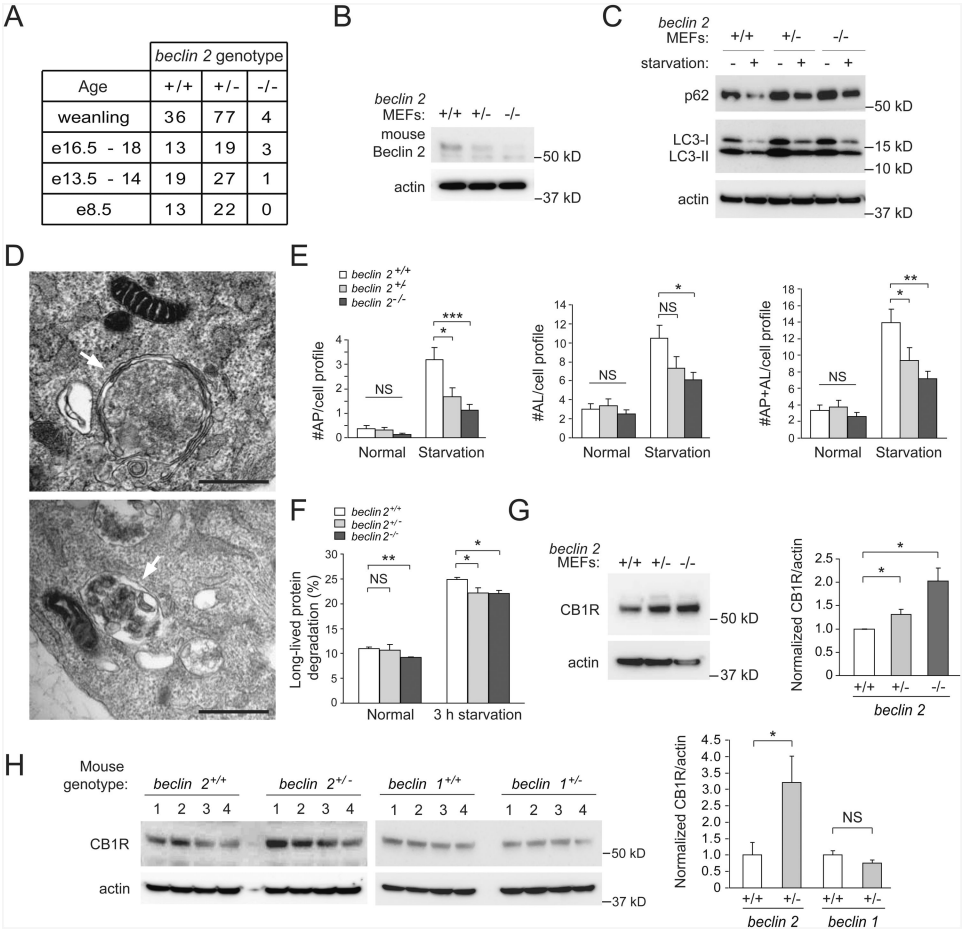

Figure 6. Role of endogenous mouse *beclin 2* in autophagy and regulation of CB1R levels

(A) Genotype distribution of offspring from *beclin 2*$^{+/-}$ intercrosses at indicated ages.

(B) Western blot detection of Beclin 2 in MEFs of indicated genotype.

(C) Western blot detection of p62 and LC3 in MEFs of indicated genotype during growth in normal medium (starvation "−") or after 3 h amino acid and serum starvation (starvation "+"). See Figure S6D for quantitative analysis of western blots from three independent experiments.

(D) Representative electron microscopic image of an autophagosome (arrow, upper panel) and an autolysosome (arrow, lower panel) in *beclin 2*$^{+/+}$ MEFs cultured for 3 h in starvation medium. Scale bars, 500 nm.

(E) Electron microscopic quantification of autophagosomes (AP) and autolysosomes (AL)in MEFs of indicated genotype cultured for 3 h in normal or starvation medium. Resultsrepresent mean ± SEM of 25 random cell profiles per experimental group.

(F) Long-lived radiolabeled cellular protein degradation in MEFs of indicated genotypecultured for 3 h in normal or starvation medium. Bars represent mean ± SEM of threeindependent experiments.

(G) Western blot detection of CB1R in MEFs of indicated genotype. Quantification of normalized levels of CB1R is shown on right. Bars represent mean ± SEM of three independent experiments.

For (E-G), *P<0.05; **P<0.01; ***P<0.001; NS, not significant; ANOVA with Dunnett Method.

(H) Western blot detection of CB1R in whole brain lysates from mice of indicated genotype. Quantification of normalized levels of CB1R is shown on right. Bars represent mean ± SEM of four mice in each genotype. *P<0.05; NS, not significant; ANOVA

See also Figure S6.

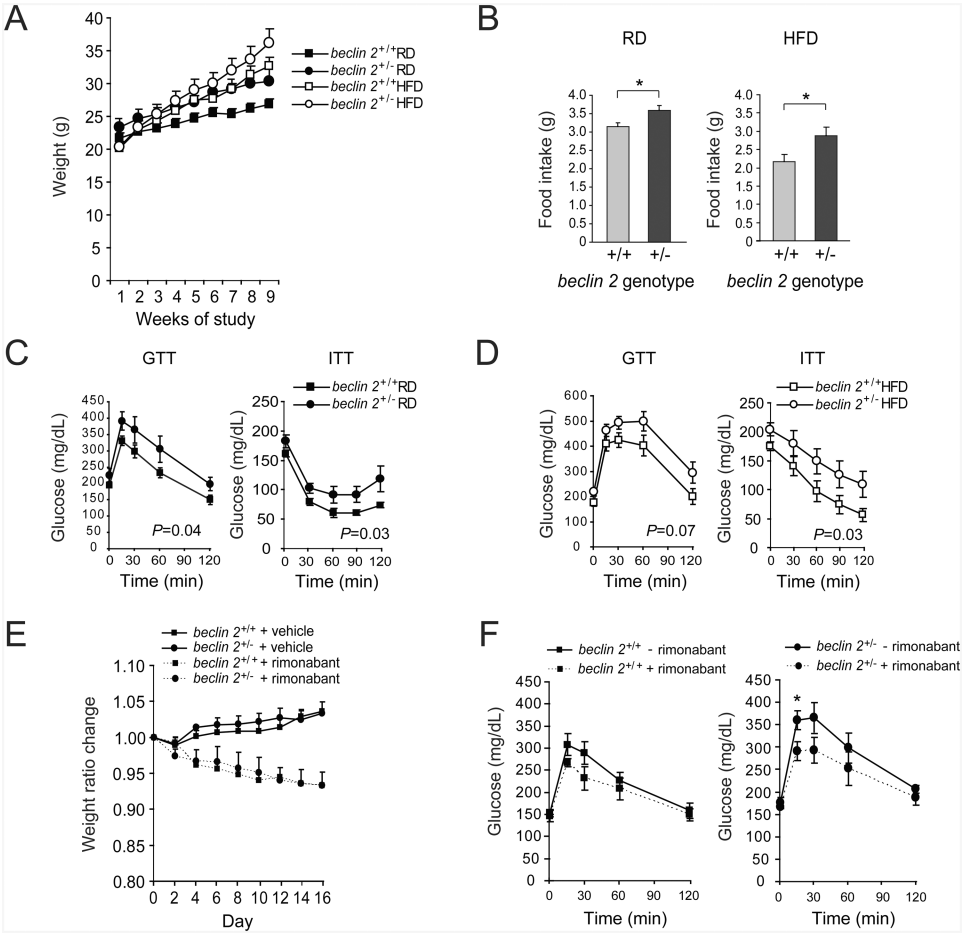

Figure 7. *beclin 2* heterozygous knockout mice develop increased body weight and insulin resistance

(A) Weekly weights of 8 week-old littermate mice of indicated genotype during 8 weeks of regular diet (RD) or high-fat diet (HFD) treatment. $P<0.001$ for *beclin* $2^{+/+}$ versus *beclin* $2^{+/-}$ in both RD and HFD conditions; linear mixed effect model.

(B) Daily food intake of littermate mice of indicated genotype at the end of 8 weeks of RD or HFD treatment. *$P<0.05$; ANOVA.

(C and D) Glucose tolerance tests and insulin tolerance tests performed on littermate mice of indicated genotype after 8 weeks RD (C) or HFD (D) treatment. *P* values in each graph represent the difference between two curves; see methods for details of statistical analysis. For (A-D), results represent mean ± SEM for 6-8 mice per experimental group.

(E) Weight ratio changes of 8 week-old littermate mice of indicated genotypes fed with RD during 16 days of daily intraperitoneal rimonabant (10 mg kg^{-1}) or vehicle control treatment. Both genotypes had similar weight ratio changes with rimonabant; *P*=NS; linear mixed effect model.

(F) Glucose tolerance tests on littermate mice of indicated genotypes fed with RD before and after 16 days of daily intraperitoneal rimonabant treatment. *$P<0.05$ for comparison of glucose value between two groups at indicated time point; ANOVA.

For (E-F), results represent mean ± SEM for 5 mice per group.

See also Figure S7.